SUPPORTING INFORMATION

The Role of Isolated Acid Sites and Influence of Pore Diameter in the Low-Temperature Dehydration of Ethanol

Matthew E. Potter,[†]* Mary E. Cholerton,[†] Julija Kezina,[†] Richard Bounds,[†] Marina Carravetta,[†] Maela Manzoli,[‡] Enrica Gianotti,[ζ] Michael Lefenfeld,[ϕ] and Robert Raja[†]*

[†]School of Chemistry, University of Southampton, University Road, Southampton, SO17 1BJ, United Kingdom
[‡]Department of Chemistry & NIS-Interdepartmental Centre, University of Turin, Via P. Guiria, 10125, Torino, Italy
[ζ]Dipartimento di Scienze e Innovazione Tecnologica, Centro Interdisciplinare Nano-SiSTeMI, Università del Piemonte Orientale, Via T. Michel 11, 15100, Alessandria, Italy
[ϕ]SiGNa Chemistry Inc, 845 Third Avenue, Suite 623, New York City, New York 10022, United States

Corresponding authors Email: M.E.Potter@soton.ac.uk, R.Raja@soton.ac.uk

Contents

Experimental details

Catalysis synthesis

The SAPO-34 and SAPO-5 synthesis were prepared according to references 1-3. Key ingredients and synthetic conditions are listed below in Table S1.

In both cases the as-prepared samples were calcined in a tube furnace under a flow of air at 575 ^{o}C for 16 hours yielding a white solid.

	SAPO-5	SAPO-34
Aluminium source	Aluminium hydroxide hydrate (Al-drich)	Aluminium isopropoxide (Aldrich)
Silicon source	Silica sol (40 wt% in H_2O, Aldrich)	Fumed silica (Aldrich)
Structure directing agent	Triethylamine (Fisher)	Tetraethylammonium hydroxide (35 wt% in H_2O, Aldrich)
Crystallization temperature/ °C	180	200
Crystallization time/ h	24	60

Table S1: Summary of synthetic conditions.

Characterisation

ICP-OES measurements were performed by Medac.

Phase purity and crystallinity of materials was confirmed by powder X-ray diffraction. Powder X-ray diffraction (PXD) was carried out using a Bruker D2 Phaser diffractometer using Cu $K_{\alpha1}/K_{\alpha2}$ radiation λ = 1.5418 Å, PXD patterns were run over a 2θ rage of 5-45° with a scan speed of 3° min^{-1} and increment of 0.01°.

Scanning electron microscopy was carried out using a Jeol JSM-5910.

Catalysis

Catalysis was performed using a custom build flow reactor provided by Cambridge Reactor Design. The reactor comprised of a syringe pump, laptop computer, two mass flow controllers, reactor with heater and control box. A 224 mm quartz reactor tube (4 mm id, 6 mm od) with a 4 mm high frit 80 mm from the base of the tube and a gas inlet 25.8 mm from the top was placed inside the heater jacket. Liquid and gas flows were controlled using a Harvard Apparatus Model 33 MA1-55-3333 syringe pump and Brooks IOM585OS mass flow controller respectively and flow rates were input via computer interface.

Silicon substitution mechanisms

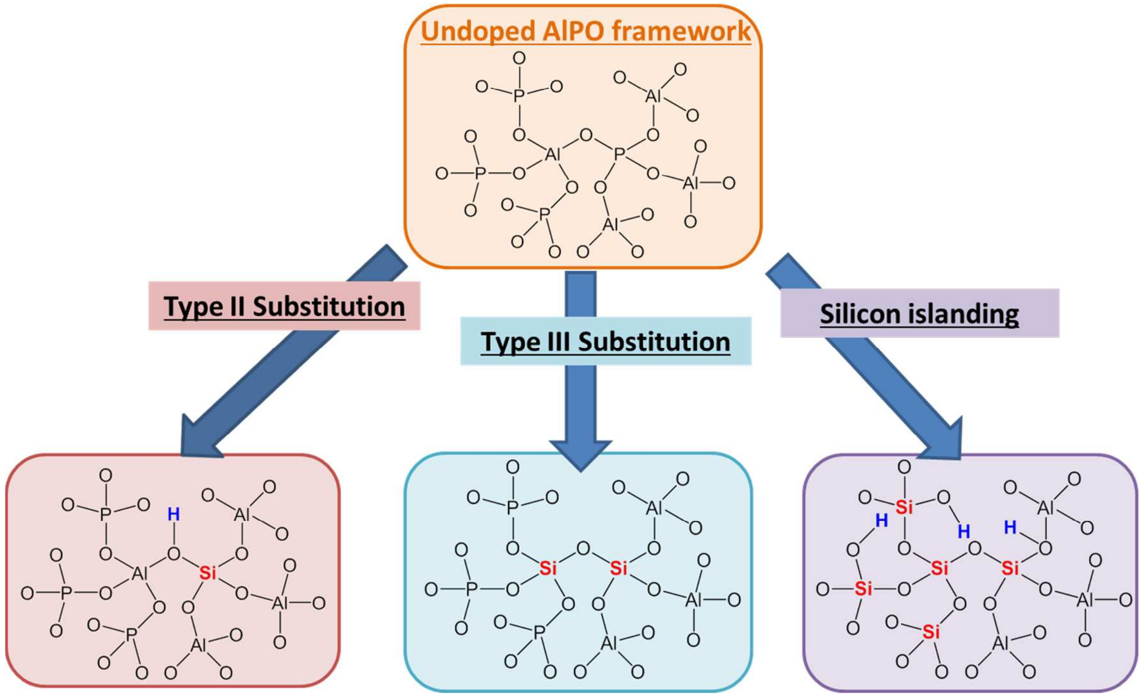

Figure S1: Possible silicon substitution methods into an AlPO framework.

Textural characterization results

Powder X-ray diffraction

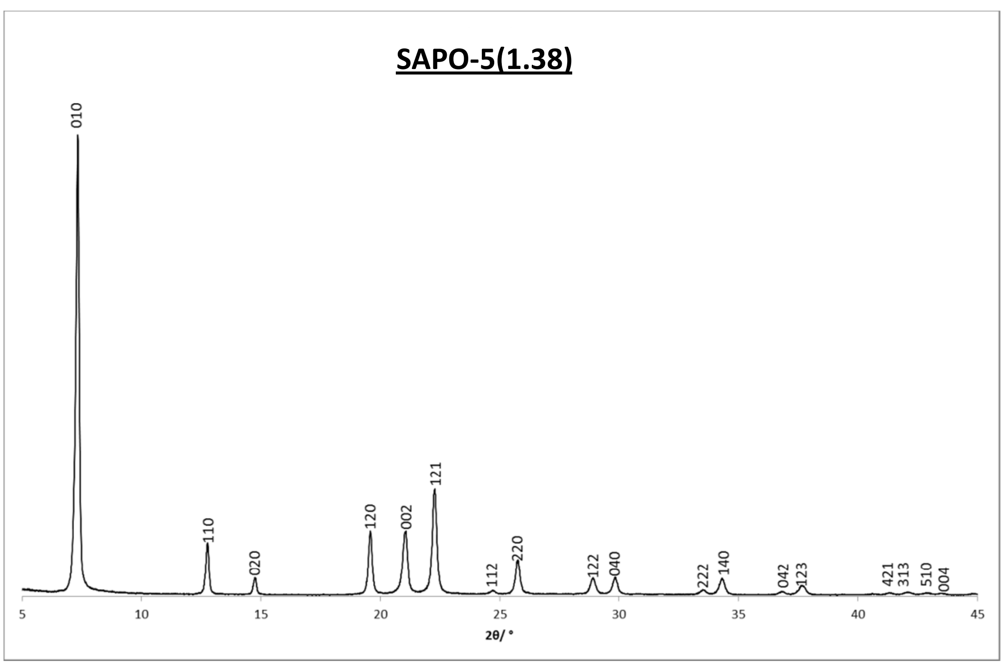

Figure S2: Powder X-ray diffraction pattern for phase-pure SAPO-5(1.38).

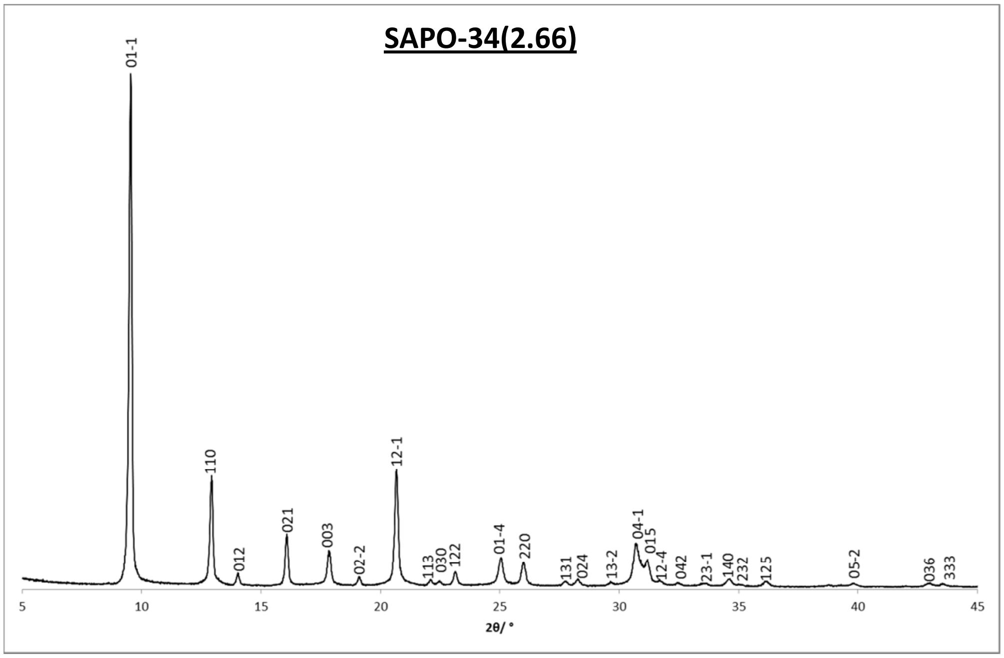

Figure S3: Powder X-ray diffraction pattern for phase-pure SAPO-34(2.66).

Catalyst	Alpha/ Å	Gamma/ Å	Volume/ Å^3
SAPO-5(1.38)	13.8431	8.4295	1398.93
SAPO-34(2.66)	13.7097	14.9052	2426.20

Table S2: Unit cell data for SAPO-5 and SAPO-34 as determined using Celref.[4]

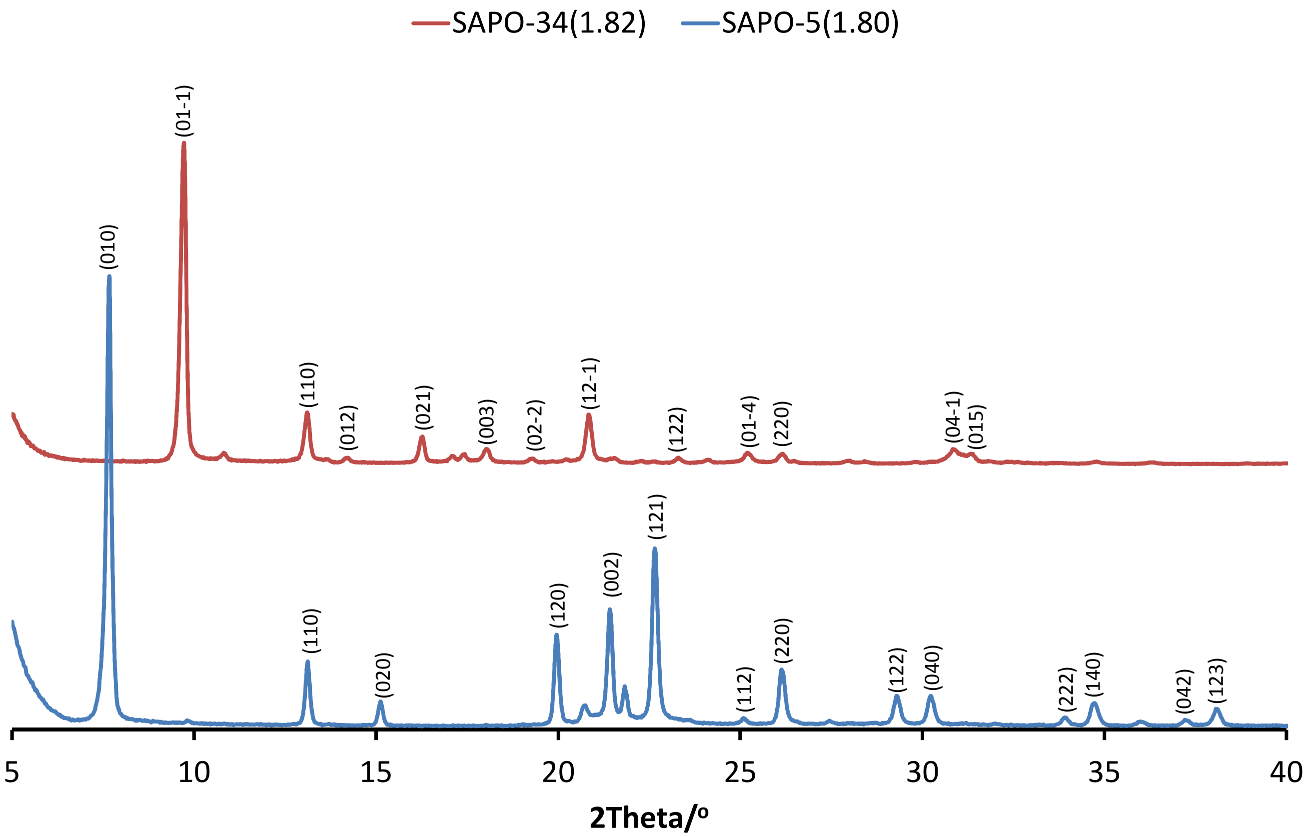

Figure S4: Powder XRD patterns for SAPO-34(1.82) and SAPO-5(1.80) showing main phase.

BET surface area measurements

	SAPO-5(1.38)	SAPO-34(2.66)
BET surface area/ m^2g^{-1}	250.98	479.37

Table S3: Surface area measurements determined using BET.

Crystallite size calculations

	SAPO-34(2.66)	SAPO-34(1.82)	SAPO-5(1.80)	SAPO-5(1.38)
Crystallite size/nm	58	43	59	50

Table S4: Crystallite sizes derived from powder-XRD with Scherrer's equation.

Scanning Electron Microscopy

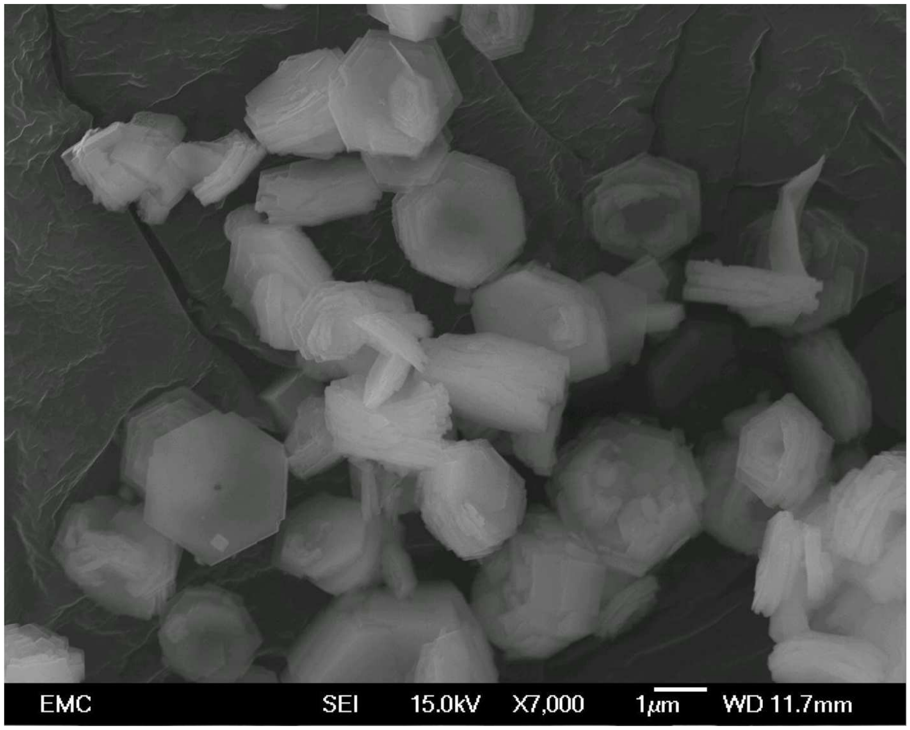

Figure S5: SEM image of SAPO-5(1.38).

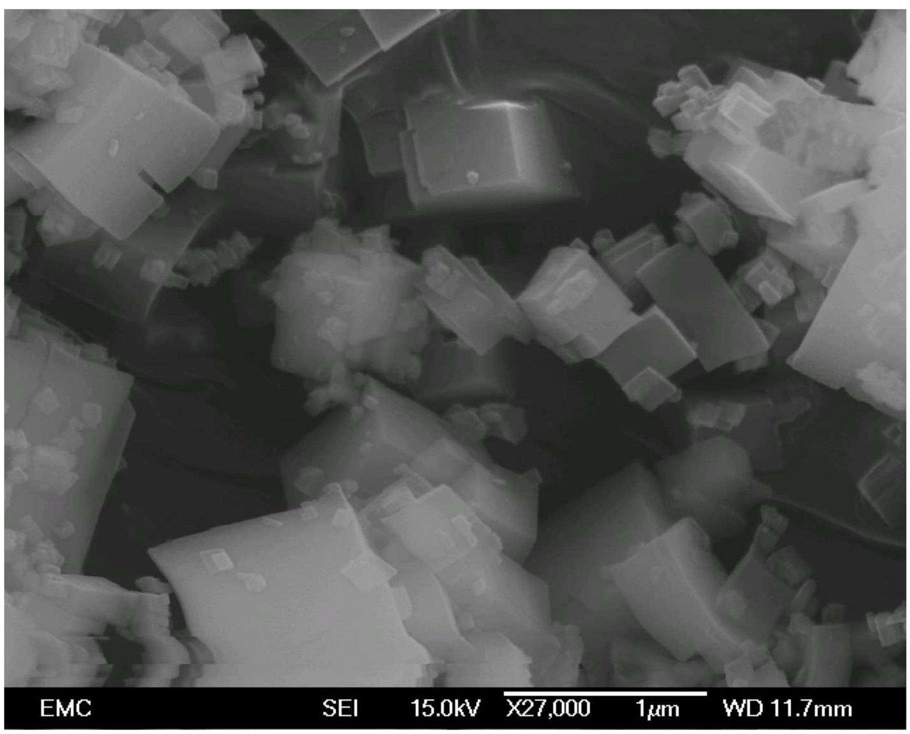

Figure S6: SEM of SAPO-34(2.66).

Probe-based FTIR spectroscopy

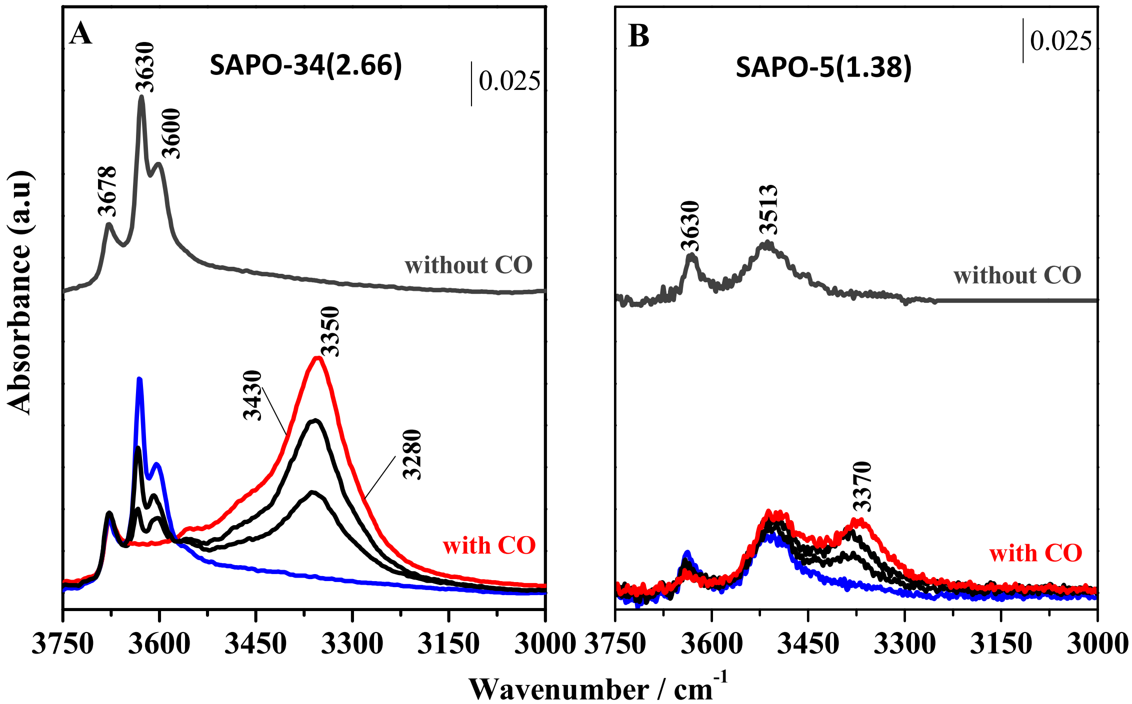

Figure S7: FTIR spectra in the OH stretching region of CO adsorbed at 80 K on calcined SAPO-34(2.66) (A) and SAPO-5(1.38) (B). Decreasing CO coverages from 30 (red curves) to 0.01 (blue curves) mbar. The spectra in vacuo before CO adsorption are also reported (grey curves).

NMR spectra

^{29}Si MAS NMR of SAPO-34(2.66)

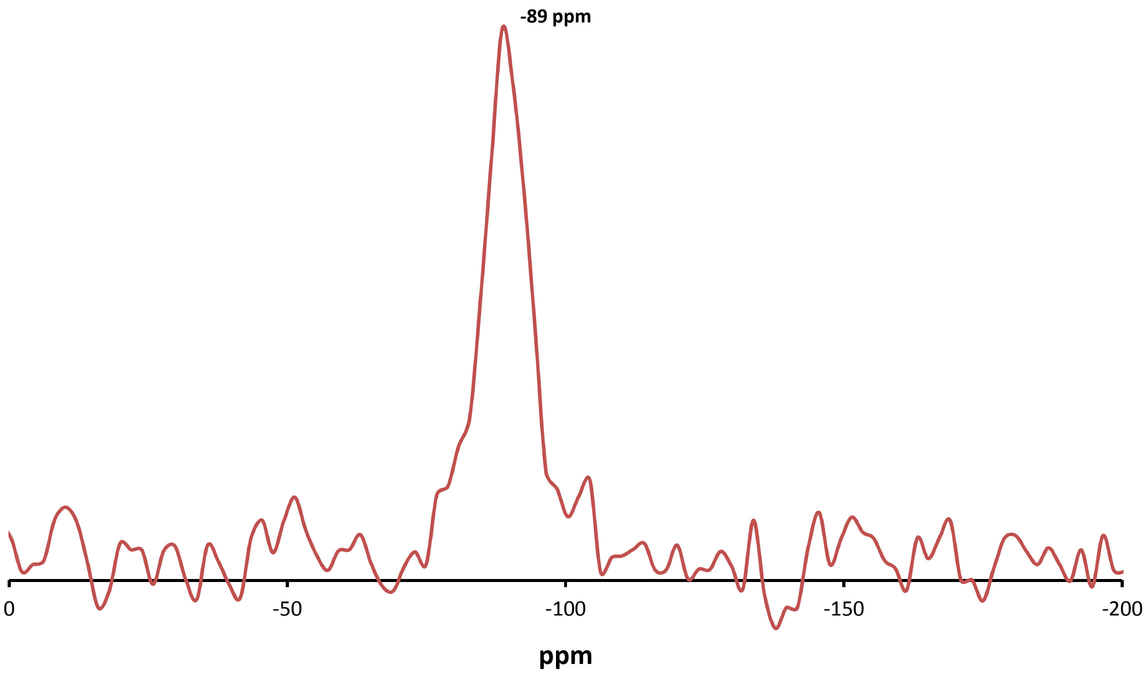

Figure S8: CP-RAMP ^{29}Si MAS NMR spectra of SAPO-34(2.66) at 9.4 T, 8 kHz spin rate. The spectrum is the result of 15000 scans.

^{29}Si MAS NMR of SAPO-5(1.38)

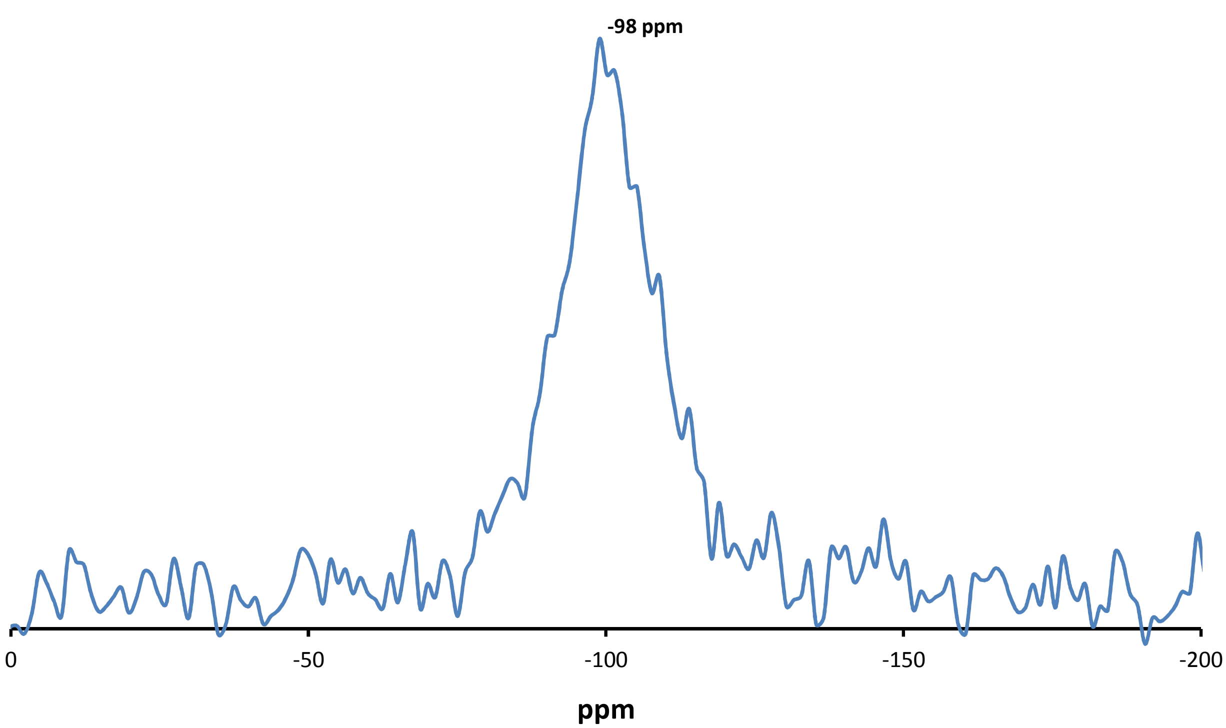

Figure S9: CP-RAMP ^{29}Si MAS NMR spectra of SAPO-5(1.38) at 9.4 T, 8 kHz spin rate. The spectrum is the result of 25000 scans.

Computational Analysis

Binding studies were also performed with NH_3 and ethanol on the specific sites witnessed by ^{29}Si NMR, to gain an insight into the acidic nature of the specific active sites and the mechanistic implications; the following equation was used to quantify the degree of interaction with the probe molecules:

(4) $\Delta_{Binding} = E[Probe + SAPO] - E[Probe] - E[SAPO]$

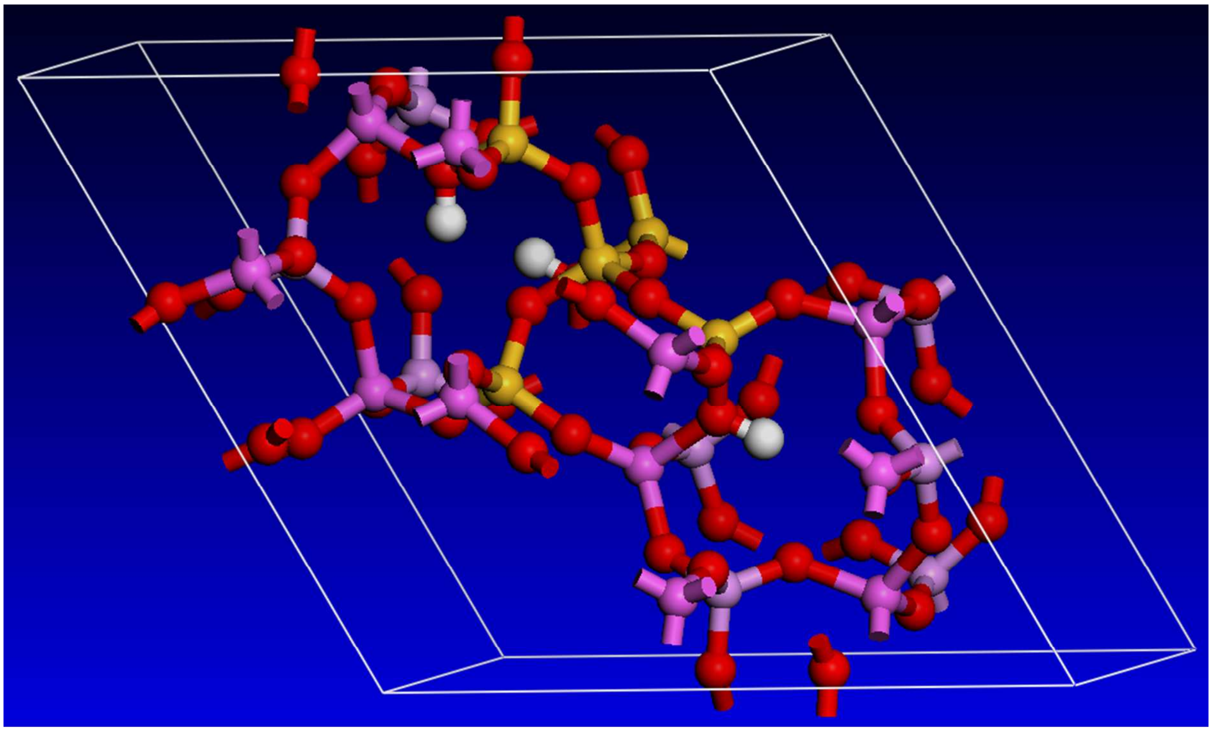

Figure S10: Optimised geometry of the 5-silicon island in SAPO-5.

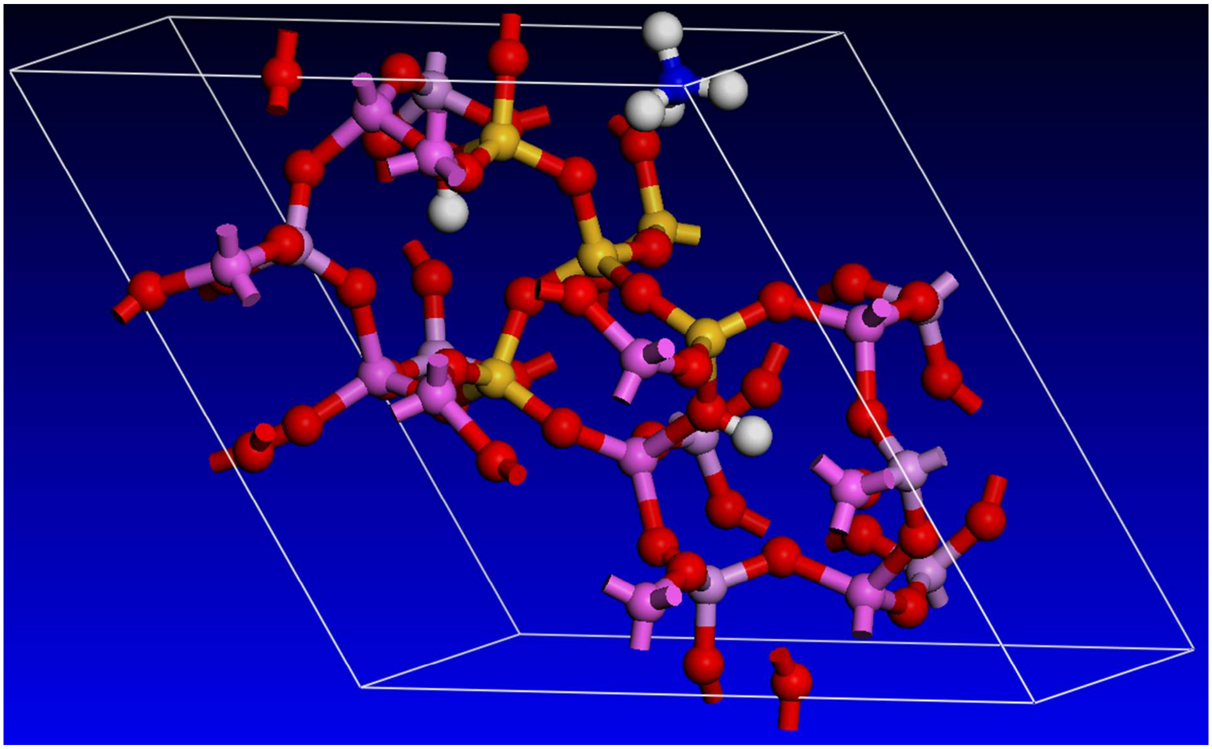

Figure S11: Optimised geometry of the binding of NH_3 to the 5-silicon SAPO-5 species.

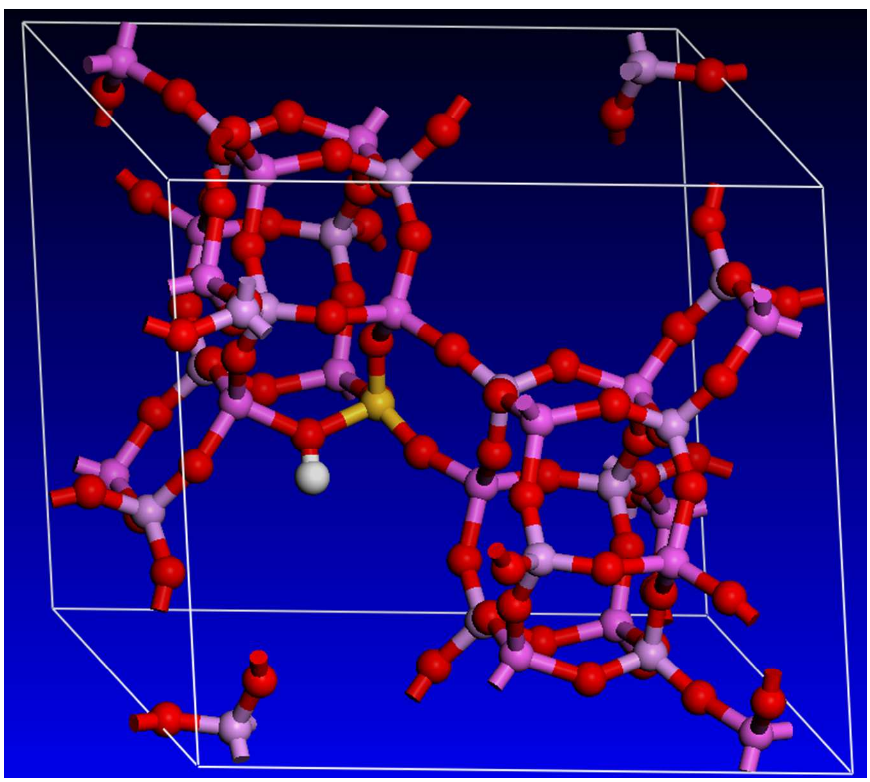

Figure S12: Optimised geometry of the isolated silicon site in SAPO-34.

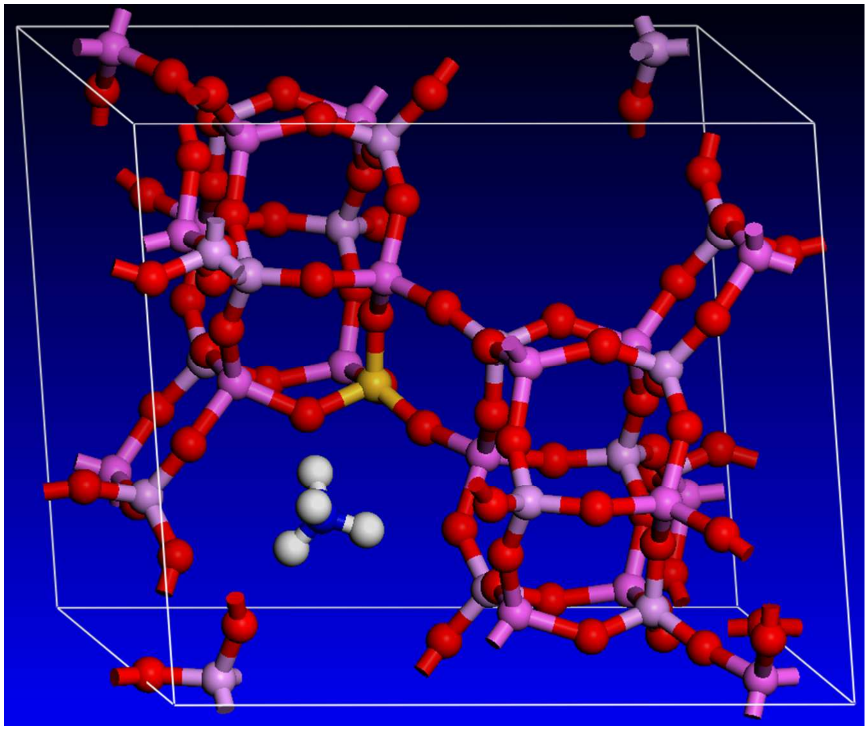

Figure S13: The optimised geometry of the isolated silicon site in SAPO-34 binding to NH_3.

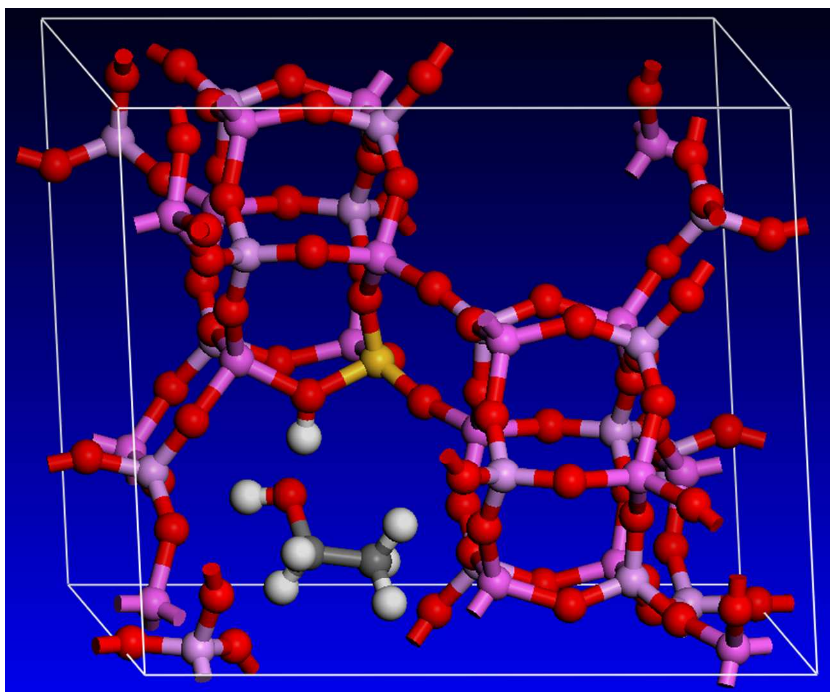

Figure S14: The optimised geometry of the isolated silicon site in SAPO-34 binding to ethanol.

Additional catalytic data

Catalyst	Conversion/mol%			Selectivity/mol%		
	300 °C	275 °C	250 °C	300 °C	275 °C	250 °C
SAPO-5(1.38)	96	89	87	94	54	31
SAPO-34(2.66)	100	98	93	100	95	76
Blank (No catalyst)	0.3	0.3	0.3	20.8	25.3	0.0

Table S5: Catalytic data for dehydration of ethanol to ethylene. WHSV = 4.38 h^{-1}, He carrier gas 50 mL min^{-1}, 0.3 g catalyst. Blank reaction performed using comparable flow rates.

References

[1] Lefenfeld, M.; Raja, R.; Paterson, A. J.; Potter, M. E. WO Patent, 2010, WO/2010085708.

[2] Lefenfeld, M.; Raja, R.; Paterson, A. J.; Potter, M. E. US Patent, 2014, US 8,759,599 B2.

[3] Lefenfeld, M.; Raja, R.; Paterson, A. J.; Potter, M. E. EU Patent, 2010, EP2389245-A2.

[4] Celref, version 3; LMGP (Laboratoire des Materiaux et du Génie Physique de l'Ecole Supérieure de Physique de Grenoble) Suite for Windows: Grenoble, 2000.